Solitons, polarons, and excitons in polyacetylene: Step-potential model for electron-phonon coupling in π-electron systems

Christoph Kuhn
Institut für Theoretische Physik, Eidgenössische Technische Hochschule–Zürich, CH-8093 Zürich, Switzerland
(Received 3 February 1989)

The bond lengths in π-electron systems, determined by electron-phonon coupling, are calculated by using a simple step-potential model. The geometry of a system is obtained by finding the self-consistency between bond length and π-electron density in the middle of each bond. The model has no free parameter and leads to a satisfactory description of unsaturated hydrocarbon chains and rings and of defect states in *trans*-polyacetylene (kinks, polarons, bipolarons, and excitons). For defect-free *trans*-polyacetylene, the calculated bond-length alternation of 0.08 Å is in close agreement with x-ray data and gives a band gap of 1.34 eV. Kinks in odd-numbered systems show hyperbolic-tangent defect geometry and have an extent of 12–18 sites, depending on the charge. Proceeding from negatively charged to neutral to positively charged kinks, the intergap state shifts towards the conduction band. Polarons created from the ground state by adding or subtracting one electron are bound and have an extent of 20–24 sites, depending on the charge. Bipolarons created from the ground state by adding or subtracting two electrons are not bound and convert, by electron-phonon coupling, to a kink ($K^{\pm}$) and an antikink ($\bar{K}^{\pm}$) pair with equal charge. Excitons created by excitation of the ground state are not bound and convert to a neutral $K^0\bar{K}^0$ pair.

I. INTRODUCTION

Soliton excitation in polyacetylene is the subject of a great number of papers, based on Hückel-type approximations[1–7](for reviews, see Refs. 8 and 9). The electron-lattice displacement is considered by minimizing the sum of electronic energy and lattice-distortion energy. Electron correlation is neglected, but considered in some papers based on the Hubbard-model approximation.[10–13] A disadvantage of Hückel-type approximations is their dependence on adjustable parameters due to their basis set which is limited to one atomic orbital per site.[14] It is of interest to consider a model which solves the one-electron Schrödinger equation in a strongly simplified potential which does not depend on free parameters, and to compare its results with the known results of linear combination of atomic orbitals (LCAO) approximations. The model, by its simplicity, emphasizing only the salient physical factors, should be useful for extensions to more complex systems.

The π electrons can be considered as electrons in a three-dimensional potential $V(x,y,z)$, appropriately constructed for known geometry by superimposing atomic contributions. The molecular lattice is in the (x,y) plane. The problem of solving the three-dimensional, one-particle Schrödinger equation can be reduced to solving the two-dimensional Schrödinger equation in an effective potential $V(x,y)$, or by solving the one-dimensional Schrödinger equation in the effective potential $V(s)$, where s is the coordinate along the bonds in the chain.[15–17] $V(x,y)$ and $V(s)$ are constructed from atomic contributions obtained by considering electron-electron interaction implicitly and taking into account the effects of side compression in decreasing distances between nuclei. The π-electron density distribution is calculated by summing the contribution of the occupied states. The following two features of the models are important.

(a) The π-electron density in the middle of the bond, ρ, and the corresponding experimental bond length d are related to each other: the π-electron charge in the bond attracts the σ-bonded nuclei by Coulomb forces and thus reduces the carbon-carbon distance, while the Coulomb repulsion of the carbon ions diminished by the shielding of the σ electrons counteracts this. The equilibrium density ρ is computed for the molecules with known bond lengths. An empirical correlation function $\rho(d)$ with its inverse $d(\rho)$ is obtained.[17]

(b) To calculate the molecular geometry of a molecule with M bonds of unknown lengths, an arbitrary configuration of bond lengths $d_1,d_2,\ldots,d_M$ is chosen and the π-electron density in the middle of each bond $\rho_1,\rho_2,\ldots,\rho_M$ is computed. $d(\rho)$ gives a new configuration of bond lengths, initiating a new cycle of an iteration process that converges to self-consistency between densities $\rho_1,\rho_2,\ldots,\rho_M$ and bond lengths $d_1,d_2,\ldots,d_M$.[17–19]

This procedure leads to bond lengths and absorption energies that are in good agreement with experimental data,[20] e.g., to a band gap of 1.3 eV, a valence-band width of 3.9 eV, and an ionization energy of 5.5 eV in the case of the infinite polyene.[16] In essence, the correlation of bond length and π-electron density in the bond is used rather than the energy-minimum method to find the bond-length pattern. This approach is along the lines of an early explanation of the bond-length alternation in polyenes by the formation of a charge-density wave leading to an instability in the chain of equal bonds.[21] Before, it was assumed that such a chain of equal bonds is the stable configuration in long polyenes. The effect was later discussed in the general case of a one-dimensional metal

suffering a periodic lattice distortion.[22]

A simplified model can be considered in which the potential troughs at the atoms are neglected for simplicity, thereby accentuating the nature of the potential between the atoms.[23] In the present paper the strongly idealized potential consists of equidistant steps at levels determined by an iteration process converging to self-consistency. Considering the potential troughs at the atoms leads to density maxima at the atoms but does not appreciably change the band structure and the charge-density waves on bonds or sites and hence does not change the molecular geometry. This is shown for butadiene (Fig. 1). The π-electron densities [Figs. 1(b) and 1(d)] resulting from the models in Figs. 1(a) and 1(c), respectively, are almost identical [the "double bonds" C(1)=(C)(2) and C(3)=C(4) are short and have high density; the "single bond" C(2)—C(3) is long and has low density], except that the density maxima on the atoms are naturally not represented by the step-potential model. This justifies the simplifying assumptions. These are further supported by pseudopotential theory.[24–26]

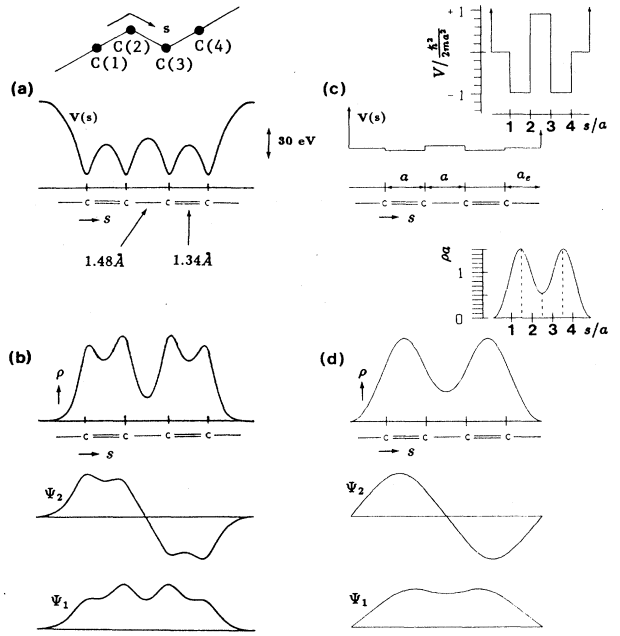

FIG. 1. One-dimensional model of butadiene. (a) Exact one-dimensional pseudopotential from the literature. The potential is composed of atomic contributions. The potential between atoms is lower for shorter distances. (b) Wave functions ψ_1 and ψ_2 of occupied states obtained by solving the Schrödinger equation for the potential in (a) and π-electron density distribution ρ of the four π electrons in ground state. Density maxima are at the carbon atoms. Density between atoms is higher for shorter distances. C(1)=C(2) and C(3)=C(4) are "double bonds," C(2)—C(3) is a "single bond." (c) Simplified step potential used in this paper. Potential steps are of length a. The termination length $a_e=0.9a$ is fixed to zero potential. Potential between atoms is lower for shorter distance (see inset). Potential troughs of carbon atoms are neglected. (d) Wave functions ψ_1 and ψ_2 of occupied states obtained by solving the Schrödinger equation for the potential in (c) and π-electron density distribution ρ of the four π electrons in the ground state. High density at double bonds C(1)=C(2) and C(3)=C(4), low density at single bond C(2)—C(3). The density in the middle of a bond (dashed lines inset) is a measure of the bond length. No density maxima are at the carbon atoms.

In the present paper, solitonic excitations in polyacetylene are studied on the basis of the step-potential model, starting with short polyenes, polymethines, and annulenes. The results essentially agree with those given in previous work.[1–7,27] This is remarkable considering the simplicity and transparency of the model avoiding adjustable parameters. Thus the model should be useful in treating large π-electron systems and soliton dynamics. Extensions of the model that include electron-electron correlation explicitly can be possibly executed with ease.[28]

II. METHOD OF CALCULATION

The potential in the middle of the single bond and the double bonds in butadiene [$d=1.48$ and 1.34 Å,[29] see Fig. 1(a)] and in the middle of the equal bonds in benzene [$d=a=1.40$ Å (Ref. 30)] taken from the one-dimensional refined pseudopotential model[28] is used to define the levels in the step-potential model [Fig. 1(c) and inset of Fig. 1(c); the unit of energy $\hbar^2/2ma^2=1.944$ eV]. We find from Fig. 1(c), for the double bonds C(1)=C(2) and C(3)=C(4), $d=0.957a$ and $V=-0.98\hbar^2/2ma^2$; for the single bond C(2)—C(3), $d=1.057a$ and $V=+0.91\hbar^2/2ma^2$. For the equal bonds in benzene, $d=a$ and $V=0$. $V(d)$ is obtained by quadratic interpolation:

$$V/(\hbar^2/2ma^2)=19.9(d/a-1)-68.3(d/a-1)^2 . \quad (1)$$

The π-electron densities ρ in the middle of the bonds of butadiene [Fig. 1(d) and inset of Fig. 1(d)] and benzene calculated with the step-potential model are the following: in butadiene, for double bonds C(1)=C(2) and C(3)=C(4), $d=0.957a$ and $\rho=1.503/a$; in butadiene, for a single bond C(2)—C(3), $d=1.057a$ and $\rho=0.533/a$; in benzene, for equal bonds, $d=a$ and $\rho=1/a$. $\rho(d)$ (Ref. 31) is obtained by quadratic interpolation:

$$\rho a=1.00-10.2(d/a-1)+35.0(d/a-1)^2 . \quad (2)$$

From Eqs. (1) and (2) (or from the ρ and V values given above) we obtain $V(\rho)$ (the quadratic term turns out to be zero),

$$V/(\hbar^2/2ma^2)=\alpha(1-\rho a), \quad \alpha=1.95 . \quad (3)$$

The numerical procedure to solve the Schrödinger equation with a potential of piecewise constant steps is outlined in the Appendix. The iteration process is sketched for butadiene and benzene [Fig. 2(a)]. Starting with any configuration of bond lengths for a π-electron system with unknown bond lengths (e.g., with equal bond lengths for butadiene), then solving the Schrödinger equation (particle in a box in this case) and calculating the π-electron density distribution, Eq. (3) gives a new configuration of steps. Solving the Schrödinger equation for this potential initiates a new cycle of the iteration. The process is continued until convergence to self-

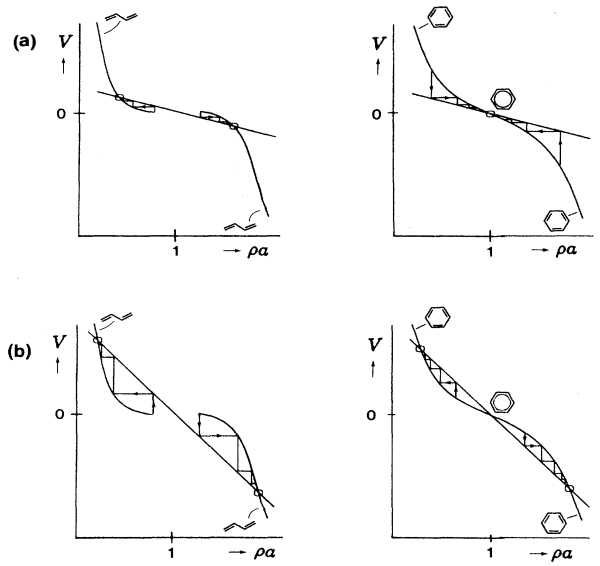

FIG. 2. Iteration process for step-potential model. Step potential V vs ρa, ρ density is in the middle of a bond. Dependence sketched for geometry of butadiene (left) and for benzene (right) with unknown step configuration. Curved line: ρ computed for given geometry (given V). Straight line with slope α: Eq. (3); α given by strength of electron-phonon coupling. Arrows: course of iteration to consistency (circles). (a) $\alpha<2.6$: convergence to bond-length alternation in case of butadiene and convergence to equal bonds in case of benzene. (b) $\alpha>2.6$: convergence to bond-length alternation in butadiene and benzene. The configuration of equal bonds in benzene is unstable.

consistency. The desired molecular geometry follows from the final configuration of steps by the inverse of Eq. (1).

In the case of benzene, starting with bond alternation, the procedure converges to equal bond lengths, demonstrating self-consistency. This finding is not trivial; for a coupling constant $\alpha>2.6$, sufficiently greater than the value $\alpha=1.95$, equal bonds in benzene would be unstable and the iteration process would converge to bond alternation [Fig. 2(b)].

LCAO treatments with their particular assumptions lead to bond-length alternation in polyacetylene but do not lead unambiguously to bond equality in benzene since a different choice of adjustable parameter values results in bond-length alternation.[6]

III. RESULTS AND DISCUSSIONS

A. Polyenes: $H(-\underset{H}{C}=\underset{H}{C}-)_nH$

Polyenes are chains with an even number $j=2n$ of carbon atoms. The smallest polyene is butadiene ($n=2$) discussed above. It has a bond-length alternation of $\Delta d=0.14$ Å, where Δd is the difference of bond lengths between the two adjacent bonds $\Delta d=(-1)^i(d_i-d_{i-1})$, and d_i is the bond length of the bond between sites i and $i+1$. For the longer polyenes (Fig. 3 for $n=15$) the alternation gets smaller, down to $\Delta d=0.08$ Å in the mid-

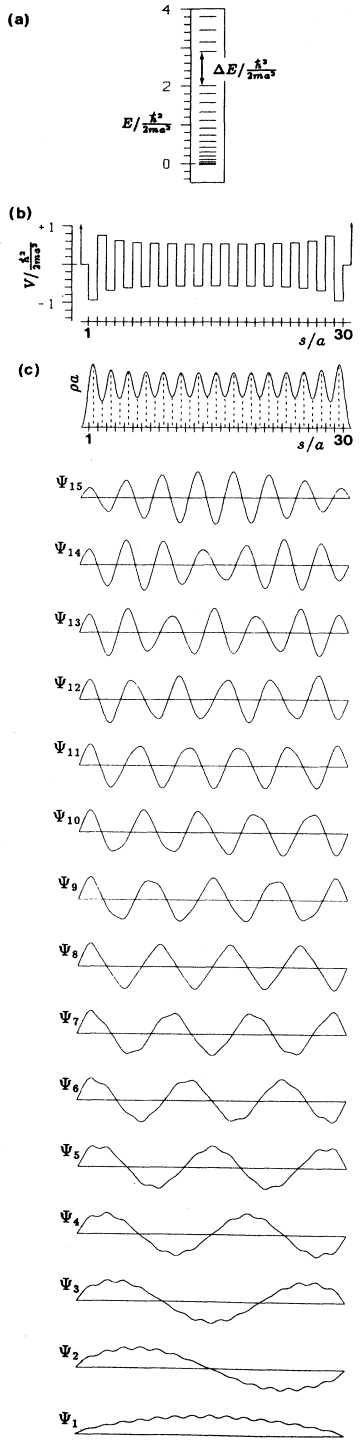

FIG. 3. Polyene: $H(-\underset{H}{C}=\underset{H}{C}-)_nH$. Case $n=15$. Number of C atoms $j=2n=30$. (a) Energy spectrum. Energy difference between lowest unoccupied state and highest occupied state $\Delta E=1.73$ eV. (b) Step potential. (c) Wave functions $\psi_1-\psi_{15}$ of occupied states. π-electron density distribution ρa. Dashed lines denote the middle of bonds. The charge-density wave is over bonds. Single- and double-bond alternation stronger at ends.

dle of the molecule. There is a termination effect at the ends of the molecule resulting in a stronger bond-length alternation $\Delta d = 0.13$ Å similar to butadiene. The π-electron density distribution shows a charge-density wave over the bonds [dashed lines in Fig. 3(c)]. The wave function of the highest occupied state [ψ_{15} in Fig. 3(c)] has maxima and minima at the double bonds and therefore this state is energetically more favorable as compared to the lowest unoccupied state. Hence a gap [Fig. 3(a)] in the energy spectrum appears.[32]

B. Polymethines: $H_2C{=}\underset{H}{C}{-}(-\underset{H}{C}{=}\underset{H}{C}-)_n-\overset{\ominus}{C}H_2$

Polymethines are chains with an odd number $j = 2n + 3$ of carbon atoms. In contrast to polyenes, where the π-electron density distribution is insensitive to variations in the termination length a_e, a change in a_e has a surprising effect for the polymethines (Fig. 4): Taking $a_e = 1.5a$ there are equal bonds (particle-in-a-box case) up to $n = 11$ with the charge-density wave over the sites. For larger values of n the bond equality is found to be restricted to the central region of the molecule. The bond-length alternation is strong towards the ends of the chain, since the π-electron density distribution changes to a charge-density wave over the bonds. The relatively abrupt transition with increasing n from bond equality to bond alternation with kinklike topology is remarkable and is contrasted to the case $a_e = 0.9a$, where the kinklike topology can be recognized even in small systems.[33]

C. Annulenes

Annulenes are rings with an even number j of carbon atoms. The Hückel rule states that $(4n+2)$-annulenes have no bond-length alternation whereas $4n$-annulenes have bond-length alternation.

It is well known that the Jahn-Teller effect causes a spontaneous dimerization for $4n$-membered ring systems with any strength of electron-phonon coupling, whereas $(4n+2)$-membered ring systems only dimerize for sufficiently large electron-phonon coupling. In the case of annulenes, benzene has equal bonds and large $(4n+2)$ annulenes must dimerize since polyenes dimerize and an infinite polyene chain is not to be distinguished from an infinite polyene ring. The maximum value n for a $(4n+2)$-annulene to have equal bonds was calculated to be between $n = 1$ (Ref. 34) to $n = 7$.[35] The SSH model with appropriate parameter values gives the value $n = 3$.[6] The approach mentioned in the Introduction leading to dimerization of polyenes[15,18,19] gives the value $n > 5$ without adjustable parameters.[17] NMR experiments show that the 14-annulene has a ring current whereas the 22-annulene has no ring current,[36] suggesting n between 3 and 4. Our result is $n = 3$ (Fig. 5). Note that this result does not depend on adjustable parameters.

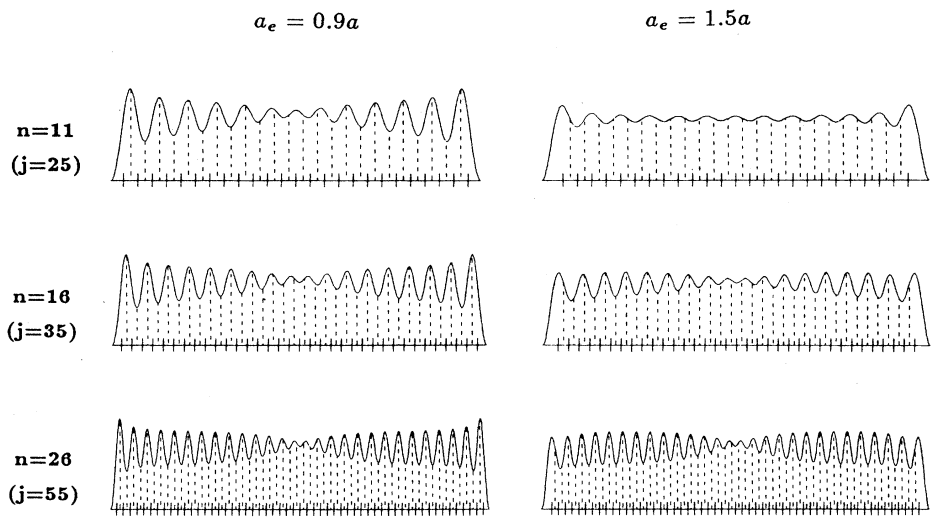

FIG. 4. Polymethines: $H_2C{=}\underset{H}{C}{-}(-\underset{H}{C}{=}\underset{H}{C}-)_n-\overset{\ominus}{C}H_2$. π-electron density distribution along molecule with $j = 2n + 3$ C atoms for three cases $n = 11, 16, 26$ and with two values of the termination lengths, $a_e = 0.9a$ and $a_e = 1.5a$. Dashed vertical lines denote the middle of each bond. Slashes denote C atoms. Case $a_e = 1.5a$, $n = 11$: the charge-density wave is over sites (equal bonds). Case $a_e = 1.5a$, $n = 11$: the charge-density wave is over sites (equal bonds). Cases $a_e = 1.5a$, $n = 16, 26$ and $a_e = 0.9a$, $n = 11, 16, 26$: kinklike topology. Charge-density wave over sites at the center of molecule (weak bond-length alternation) and charge-density wave over bonds at ends of chain (strong bond-length alternation).

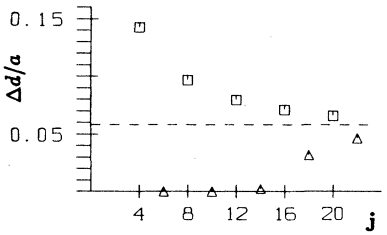

FIG. 5. $4n$- and $(4n+2)$-annulenes. Bond-length alternation $\Delta d=|d_i-d_{i-1}|$; d_i is the bond length between sites i and $i+1$. j is the number of C atoms. $(j=4n)$-annulenes (squares): strong bond-length alternation for $n=1$; bond lengths converge with increasing n to an alternation $\Delta d=0.08$ Å. $(j=4n+2)$-annulenes (triangles): bond equality for benzene and other $(4n+2)$-annulenes up to $n=3$ $(j=14)$; weak bond-length alternation at $n=4$ $(j=18)$; Δd converges with increasing n to $\Delta d=0.08$ Å.

D. Polyacetylene

1. *The ground state*

We describe the ground state of polyacetylene as a large even-numbered ring with cyclic boundary conditions to avoid the termination effects mentioned above (Secs. III A and III B). The ground state has a bond-length alternation $\Delta d=0.082$ Å and a band gap $\Delta E=1.34$ eV, in good agreement with experiments.[8,37]

2. *Kinks*

In an odd-numbered ring the two bond-length–alternation patterns

$$\ldots{=}\mathrm{C}{-}\mathrm{C}{=}\mathrm{C}{-}\mathrm{C}{=}\mathrm{C}{-}\ldots$$

and

$$\ldots{-}\mathrm{C}{=}\mathrm{C}{-}\mathrm{C}{=}\mathrm{C}{-}\mathrm{C}{=}\ldots$$

unite, forming a localized defect called a kink. The kink creates an intergap state (energy spectrum in Fig. 6). The corresponding wave function is well localized (wave function in Fig. 6 with vertical line at the center). This intergap wave function is closely related to the topology of the kink [deviation from mean bond length in Fig. 6, $i=$integer (s/a) indicating site i]. There are two different modes of a kink, weak and strong, the center of the defect being shifted by one site.[7] This is schematically represented for a weak negative kink as

$$\ldots{-}\mathrm{C}{=}\mathrm{C}{-}\overset{\ominus}{\mathrm{C}}{-}\mathrm{C}{=}\mathrm{C}{-}\ldots\ ,$$

a weak neutral kink as

$$\ldots{-}\mathrm{C}{=}\mathrm{C}{-}\dot{\mathrm{C}}{-}\mathrm{C}{=}\mathrm{C}{-}\ldots\ ,$$

and a weak positive kink as

$$\ldots{-}\mathrm{C}{=}\mathrm{C}{-}\overset{\oplus}{\mathrm{C}}{-}\mathrm{C}{=}\mathrm{C}{-}\ldots\ .$$

The wave function of the intergap state of the weak kink has an antinode at the center of the defect (vertical line at $s/a=70$). The deviation from the mean bond length d_i-a expresses the single- (double-) bond character of a bond. The two equal bonds in the center of the defect have more single-bond character than the bonds next to them.

The strong kink can be represented by mesomeric structures as follows: for a strong negative kink,

$$\ldots{=}\mathrm{C}{-}\overset{\ominus}{\mathrm{C}}{-}\mathrm{C}{=}\mathrm{C}{-}\mathrm{C}{=}\ldots \leftrightarrow \ldots{=}\mathrm{C}{-}\mathrm{C}{=}\mathrm{C}{-}\overset{\ominus}{\mathrm{C}}{-}\mathrm{C}{=}\ldots\ ,$$

for strong neutral kink,

$$\ldots{=}\mathrm{C}{-}\dot{\mathrm{C}}{-}\mathrm{C}{=}\mathrm{C}{-}\mathrm{C}{=}\ldots \leftrightarrow \ldots{=}\mathrm{C}{-}\mathrm{C}{=}\mathrm{C}{-}\dot{\mathrm{C}}{-}\mathrm{C}{=}\ldots\ ,$$

and for strong positive kink,

$$\ldots{=}\mathrm{C}{-}\dot{\mathrm{C}}{-}\mathrm{C}{=}\mathrm{C}{-}\mathrm{C}{=}\ldots \leftrightarrow \ldots{=}\mathrm{C}{-}\mathrm{C}{=}\mathrm{C}{-}\overset{\oplus}{\mathrm{C}}{-}\mathrm{C}{=}\ldots\ .$$

The wave function of the intergap state of the strong kink has a node at the center of the defect (vertical line at $s/a=69$). Its envelope is shifted by one site compared to the weak kink, while the phase is unchanged. The two equal bonds in the center of the defect have more double-bond character than the bonds next to them.

Weak and strong kinks are self-consistent solutions describing two different stable states with the center of the defect at adjacent sites. Thus the energy of a kink moving along the chain is minimal for weak and strong kinks, while intermediate states have higher energies. Considering two adjacent bonds enclosing a particular site i in the course of a kink passing over it, the single bond gradually turns into a double bond (the adjacent bond vice versa,) according to the change of the π-electron density. The bond alternation $\Delta d_i=(-1)^i(d_i-d_{i-1})$ between the two adjacent bonds proceeds from $+0.058a$ to $-0.058a$. Hence the intermediate state of a kink has to be self-consistent with the constraint of the bond alternation Δd_i fixed to a given value between the value in the weak and the strong kink enclosing the intermediate state. The transition state has a little higher energy (less than 10^{-3} eV) than the two stable states, indicating a nearly free translation of kinks through the otherwise perfect lattice. This value is similar to the kink-pinning energy calculated within the SSH model.[1]

The negative kink has two electrons, the neutral kink has one electron, and the positive kink has no electrons in this intergap state, which shifts towards the conduction-band edge when these electrons are removed. This is due to the increasing single-bond character in the range of the defect. The squares of the corresponding wave functions have the following envelopes [case of the weak negative kink in Fig. 7(a)]:

$$\text{negative kink:}\ \sim \operatorname{sech}^2(x/8.5)\ ,$$

$$\text{neutral kink:}\ \sim \operatorname{sech}^2(x/9.25)\ ,$$

$$\text{positive kink:}\ \sim \operatorname{sech}^2(x/8.2)\ ,$$

where $x=(s-s_0)/a$ and s_0 is the s value in the center of the defect. The bond-length-alternation pattern shows the topological consequences and can be approximated by [case of the weak negative kink in Fig. 7(b)]

$$\text{negative kink:}\ \Delta d=0.058a\tanh(x/8.0)\ ,$$

$$\text{neutral kink:}\ \Delta d=0.058a\tanh(x/9.0)\ ,$$

$$\text{positive kink:}\ \Delta d=0.058a\tanh(x/6.2)\ .$$

In the case of the neutral kink the lengths of the two bonds in the center of the defect are equal to the mean bond length. In the case of the negative kink the high electron density of the intergap state at the bonds [circles in Fig. 7(a)] leads to bonds with predominantly double-bond character in the region of the defect (Fig. 6), localizing the defect more strongly than in the neutral kink. Proceeding from the neutral to the positive kink, the single-bond character in the range of the defect is increased, reducing the extent of the defect more strongly than by proceeding from the neutral kink to the negative kink.

3. *Polarons*

An electron is added to the ground state of polyacetylene; then the lowest state of the conducting band is occupied with one electron. Relaxation caused by electron-phonon coupling reveals two intergap states (negative polaron in Fig. 8). The lower state is very close to the valence-band edge and filled with two electrons;

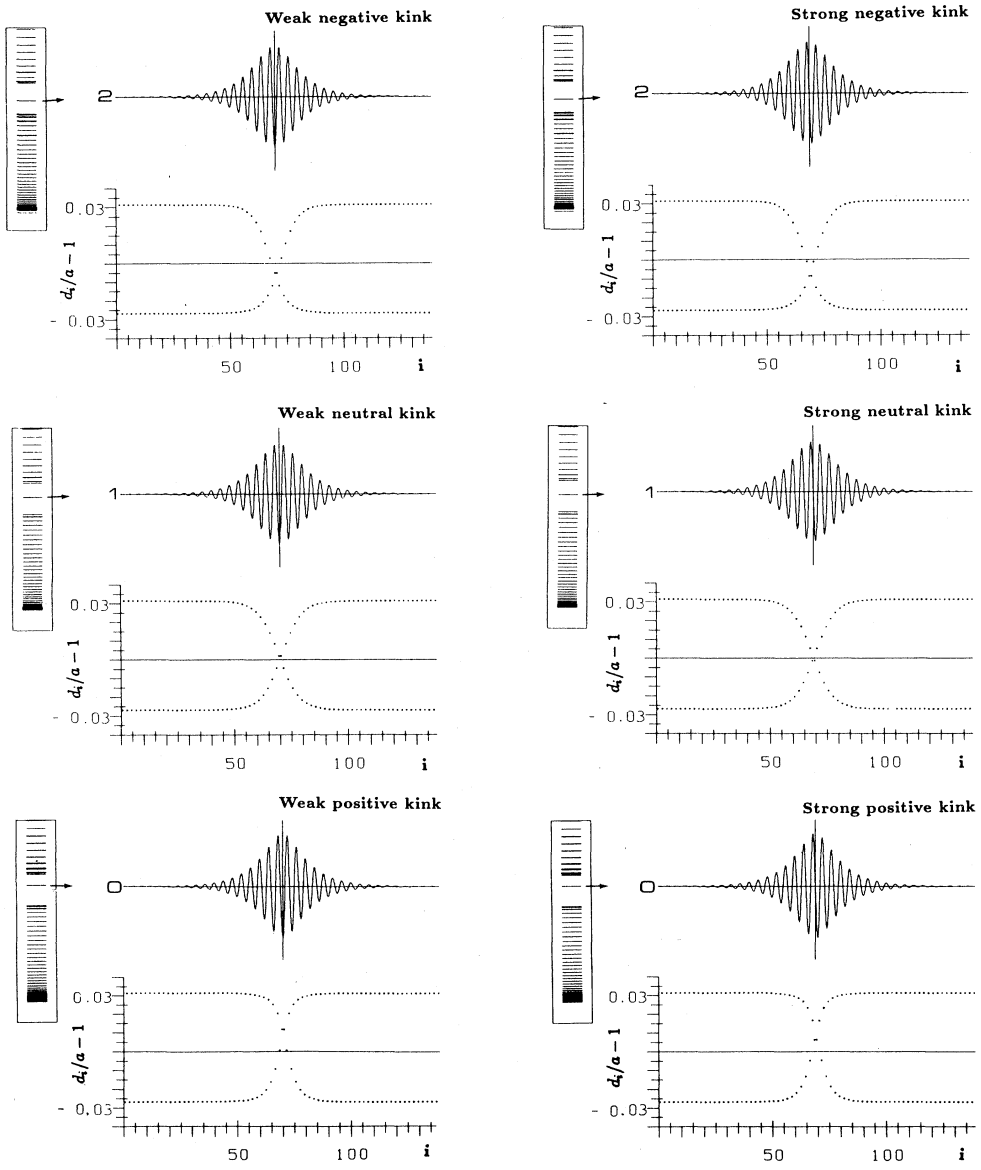

FIG. 6. Kinks. Energy spectrum; band gap $\Delta E = 1.34$ eV. The charge of the kink is given by occupation of the intergap state: negative kinks, filled intergap state (two electrons); neutral kinks, half-filled intergap state (one electron); positive kinks, empty intergap state (no electron). In proceeding from the negative kink to the neutral kink to the positive kink, the intergap state shifts towards the conduction band. The wave function of the intergap state is shown. The vertical line at the center of the defect marks the symmetry of the wave function. Weak kinks have an antinode at the center of defect ($i = 70$), strong kinks a node ($i = 69$). The deviation from the mean bond length $d_i - a$ is plotted against i, d_i is the bond length between sites i and $i+1$ and a the mean bond length. In the case of negative (positive) kinks, the bonds in the region of the defect have predominantly double- (single-) bond character. In the case of weak (strong) kinks, the bonds in the center of defect have more single- (double-) bond character than the bonds next to them.

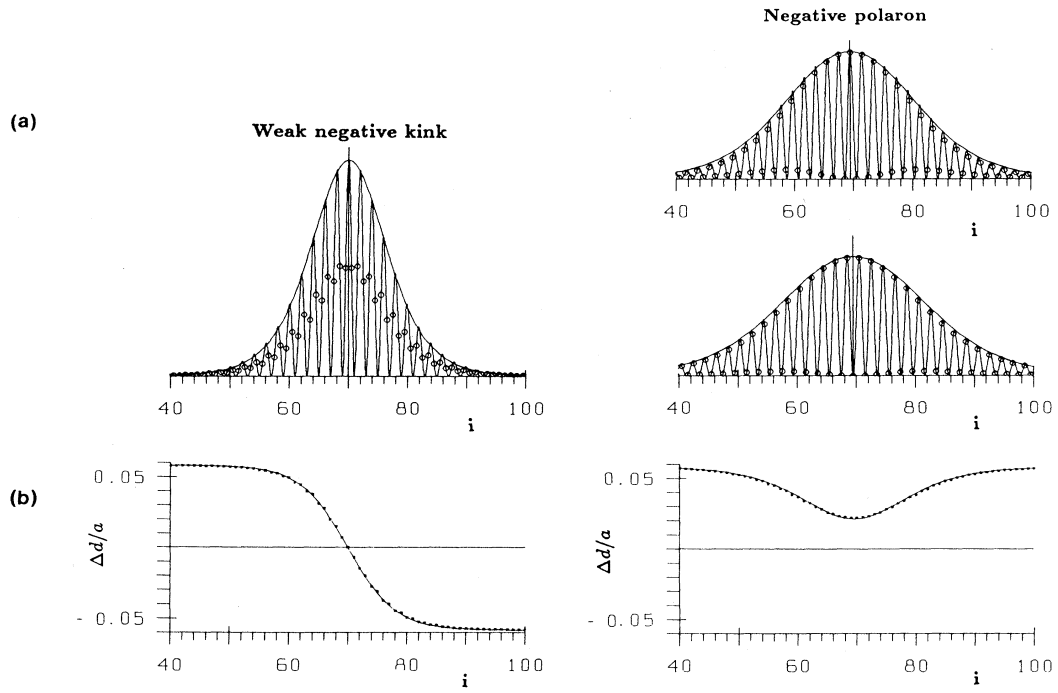

FIG. 7. Kink and polaron (Refs. 43 and 44). (a) Squares of wave functions of intergap states. Circles indicate values in middle of bonds. *Weak negative kink*: alternating maxima and zeros at sites, envelope $\sim\mathrm{sech}^2(x/8.5)$; $x=(s-s_0)/a$, $s_0=s$ at the center of the defect. *Negative polaron, upper state*: maxima (zeros) at bonds with predominantly single- (double-) bond character, envelope $\sim[\mathrm{sech}(x/12.7-0.44)+\mathrm{sech}(x/12.7+0.44)]^2$; the low-density values in the middle of bonds lie on the curve given by $\sim[\mathrm{sech}(x/12.7-0.44)-\mathrm{sech}(x/12.7+0.44)]^2$. *Negative polaron lower state:* maxima (zeros) at bonds with predominantly double- (single-) bond character, envelope $\sim[\mathrm{sech}(x/14.1-0.44)+\mathrm{sech}(x/14.1+0.44)]^2$; the low-density values in the middle of bonds lie on the curve given by $\sim[\mathrm{sech}(x/14.1-0.44)-\mathrm{sech}(x/14.1+0.44)]^2$. (b) Bond-length–alternation pattern. $\Delta d_i=(-1)^i(d_i-d_{i-1})$. Weak negative kink, $\Delta d=0.058a\tanh(x/8.0)$; negative polaron, $\Delta d=0.058a[1-0.64\,\mathrm{sech}^2(x/12)]$.

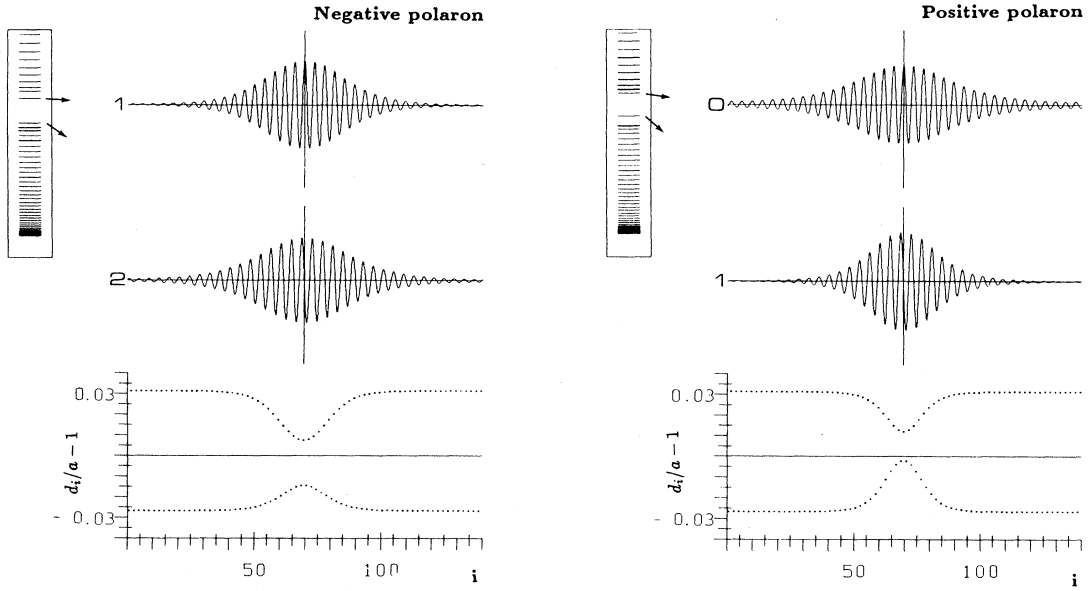

FIG. 8. Polarons. Energy spectrum. Band gap $\Delta E=1.34$ eV. Two intergap states. Negative polaron: lower state filled, upper-state half-filled. Positive polaron: lower state half-filled, upper state empty. Wave functions of the upper and lower intergap states are shown; the vertical ine at the center of the defect ($i=69.5$) marks the symmetry of the wave function. The lower state has a node at the center of the defect, the upper state an antinode. Deviation from mean bond length (d_i-a) vs i.

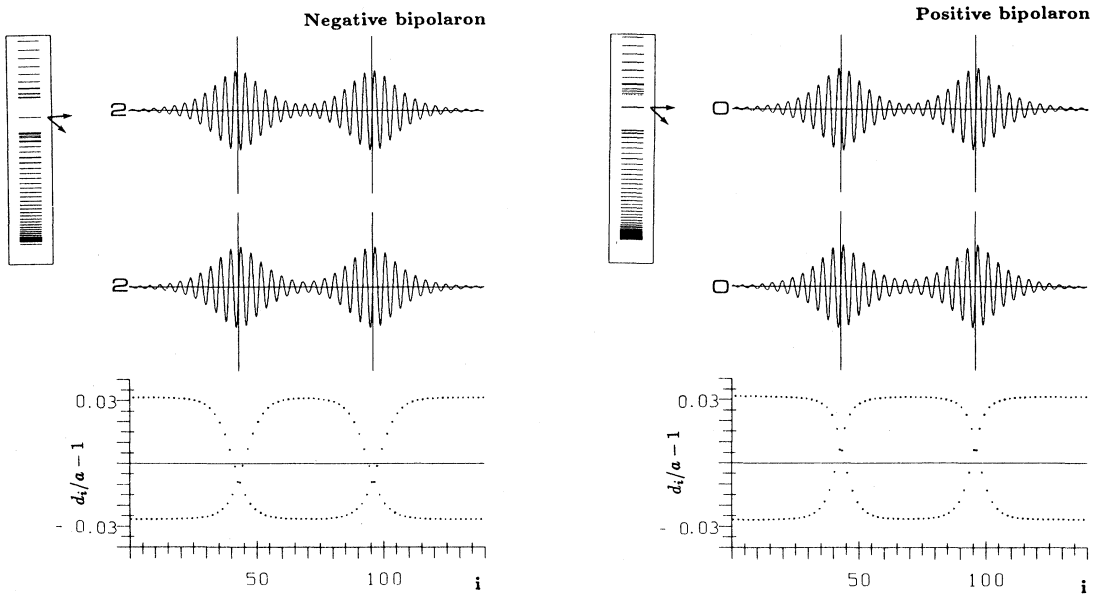

FIG. 9. Bipolarons. Energy spectrum. Band gap $\Delta E = 1.34$ eV. Two nearly degenerate intergap states. Negative bipolaron: both intergap states filled. Positive bipolaron: both intergap states empty. Wave functions of the upper and lower intergap states are shown. Two localization centers are present. Deviation from mean bond length $(d_i - a)$ vs i. Note bond alternation outside defects, inverse bond alternation in the central region, and occurrence of an equally charged kink and antikink.

the upper state is near the conduction-band edge and filled with one electron. The wave functions of these two states are well localized and the lower state is less localized than the upper state (vertical line at $s/a = 69.5$).

The squares of wave functions have the following envelopes [case of the negative polaron in Fig. 7(a)]: for the upper state,

$$\sim[\mathrm{sech}(x/12.7-0.44)+\mathrm{sech}(x/12.7+0.44)]^2 ,$$

and for the lower state,

$$\sim[\mathrm{sech}(x/14.1-0.44)+\mathrm{sech}(x/14.1+0.44)]^2 .$$

The square of the wave function of the lower state has maxima in the double bonds and zeros in the single bonds, whereas the square of the wave function of the upper state has maxima in the single bonds and zeros in the double bonds [circles in Fig. 7(a)]. The additional electron occupying the upper intergap state accumulates in the single bonds in the range of the defect and changes them to a more double-bond character. This causes a further charge-density increase in these bonds at the expense of charge density in the double bonds in the defect, forming the lower intergap state (negative polaron in Fig. 8). Thus a negative polaron is created with a bond-length–alternation pattern [case of the negative polaron in Fig. 7(b)]:

$$\Delta d = 0.058a[1-0.64\,\mathrm{sech}^2(x/12)] .$$

If an electron is subtracted from the ground state of polyactelyene, then the highest state of the valence band

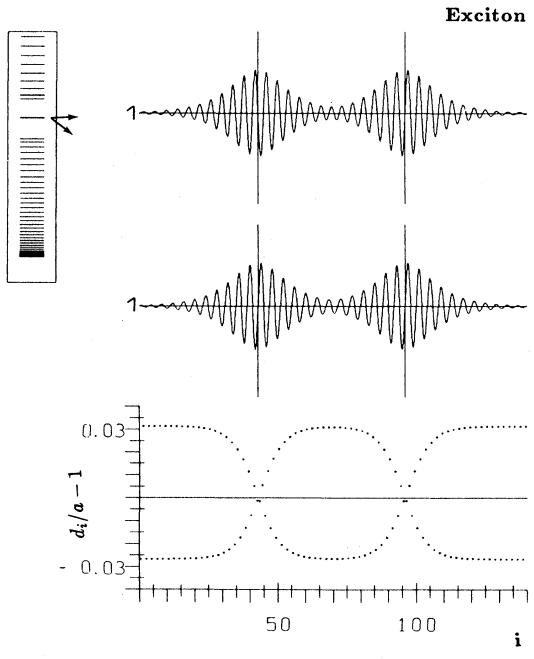

FIG. 10. Exciton. Energy spectrum. Band gap $\Delta E = 1.34$ eV. Two nearly degenerate intergap states, both singly occupied. Wave function of upper and lower intergap states are shown; two localization centers are present. Deviation from mean bond length, $(d_i - a)$ vs i. Note bond alternation outside defects, inverse bond alternation in the central region, and occurrence of a neutral kink and neutral antikink.

is occupied with one electron. Relaxation reveals two intergap states (positive polaron in Fig. 8): the lower state is near the valence-band edge and filled with one electron, and the upper state is very close to the conduction-band edge and empty. The wave functions of these two states are well localized; the lower state is more localized than the upper state (vertical line at $s/a=69.5$). The squares of the wave functions have the envelopes, for the upper state,

$$\sim[\mathrm{sech}(x/15.7-0.44)+\mathrm{sech}(x/15.7+0.44)]^2 ,$$

and for the lower state,

$$\sim[\mathrm{sech}(x/10.5-0.44)+\mathrm{sech}(x/10.5+0.44)]^2 .$$

The square of the wave function of the lower state has maxima in the double bonds and zeros in the single bonds, whereas the square of the wave function of the upper state has maxima in the single bonds and zeros in the double bonds (the same as in the case of the negative polaron). The missing electron produces a hole in the lower intergap state, which accumulates in the double bonds in the range of the defect and changes them to more single-bond character. This causes a further charge-density decrease in these bonds at the expense of the single bonds in the defect, forming the upper intergap state. Thus a positive polaron is created which, compared with the negative polaron, is more localized:

$$\Delta d=0.058a[1-0.76\,\mathrm{sech}^2(x/10)] .$$

4. *Bipolarons*

Two electrons are added to the ground state of polyacetylene; then the lowest state of the conduction band is occupied with two electrons. Relaxation reveals two nearly degenerate filled intergap states (negative bipolaron in Fig. 9), and their wave functions have two localization centers. The unbound bipolaron evolves into a well-separated negative-kink–negative-antikink pair $K^-\overline{K}^-$. Two electrons are subtracted from the ground state of polyacetylene; therefore the highest state of the valence band is empty. Relaxation reveals two nearly degenerate empty intergap states (positive bipolaron in Fig. 9), and their wave functions have two localization centers. The unbound bipolaron evolves into a well-separated positive-kink–positive-antikink pair $K^+\overline{K}^+$.

In the present approach the Coulomb repulsion of the two equally charged localization centers is neglected, which would favor the splitting of bipolarons.

5. *Excitons*

We excite the ground state of polyacetylene; then one electron is removed from the highest state of the valence band and enters the lowest state of the conduction band. Relaxation reveals two intergap states (Fig. 10). Their wave functions have two localization centers. Thus the unbound exciton evolves into a well-separated neutral-kink–neutral-antikink pair $K^0\overline{K}^{\mp}$. An oppositely charged pair $K^{\pm}\overline{K}^{\mp}$ is unstable and converts into the neutral pair in the course of the iteration process.

IV. CONCLUSIONS

We have computed the geometry and the electronic energy spectrum of molecules such as polyenes (even-numbered chains), polymethines (odd-numbered chains) and annulenes (even-numbered rings), and of defects in polyacetylene such as kinks (negative, neutral, positive), polarons and bipolarons (negative, positive), and excitons (neutral), using a step-potential model for π-electron systems. The results listed as follows essentially agree with those given in previous work, which is remarkable considering the simplicity of the model.

(a) Equal bonds in $(4n+2)$-annulenes for $n<4$.[6]

(b) Bond-length alternation in polyenes, $4n$-annulenes for $n\geq 1$, and $(4n+2)$-annulenes for $n\geq 4$.[6]

(c) Bond-length alternation in polyacetylene of $\Delta d=0.08$ Å and a band gap $\Delta E=1.34$ eV.[5,8,27,37]

(d) $\mathrm{sech}^2(x/l)$ shape of envelopes of squares of wave functions of intergap states of kinks.[1,2]

(e) $\tanh(x/l)$ shape of bond-length alternation with an extent $2l=12-18$ sites for kinks.[1,2]

(f) $[\mathrm{sech}(x/l+\beta)+\mathrm{sech}(x/l-\beta)]^2$ shape of envelopes of squares of wave functions of intergap states of polarons, $\beta=0.44$.[3]

(g) $[1-\alpha\,\mathrm{sech}^2(x/l)]$ shape of bond-length alternation with an extent $2l=20-24$ sites for polarons.[3,5]

(h) Instability of bipolarons by separation into $K^{\pm}\overline{K}^{\pm}$.[3,5,9,27]

(i) Instability of excitons by separation into $K^0\overline{K}^0$.[9,38]

Additionally, the model leads to a broken electron-hole symmetry. Electron-hole symmetry in SSH models of polyacetylene is rooted in the Hückel-type approximation with the following properties.[1–9]

(i) Symmetry of valence and conduction bands.

(ii) Midgap state in the case of the kinks independent of their charge.

(iii) Two symmetric intergap states near the band edges in the case of polarons (i.e., the distance of the lower state from the valence-band edge is the same as the distance of the upper state from the conduction-band edge independent of the charge).

(iv) Shape and extent of defect independent of its charge.

In the present approximation the intergap state of the kink is near the center of the gap, its position depending on charge. The intergap state shifts towards the conduction-band edge as one proceeds from the negative to the neutral to the positive kink. This is due to the increased single-bond character in the range of the positive kink causing an increased energy of the intergap state which is localized in this range. The charged kinks are more localized than the neutral kinks because their bonds in the center of the defect deviate from the mean bond character present in the neutral kink. Additionally, the positive kink is more localized than the negative kink.

Similarly, the two intergap states of a polaron shift towards the conduction band as one proceeds from the negative to the positive polaron, but the distances of both states from the band edges are now small. In the case of the negative polaron the lower state is closer to the valence-band edge than the upper state from the

conduction-band edge and the defect is weak and extended. In the case of the positive polaron, the lower state is further away from the valence-band edge than the upper state from the conduction-band edge and the defect is strong and localized. Boudreaux *et al.*[27] report calculations using the Dewar-Thiel modified neglect of diatomic overlap (MNDO) scheme, which also break the electron-hole symmetry. MNDO calculations give the relative positions of the gap states rather well but overestimate the electronic band gap. The intergap state of a kink is closer to the valence-band edge for the negative kink and further away for the positive kink, in accordance with our findings. Due to the larger band gap within the MNDO scheme, kinks and polarons are more localized. Negative-charged kinks and polarons are more localized compared to the positive-charged kinks and polarons; the polarons have one intergap state, in contrast to our findings.

The strongly idealized model presented in this paper neglects all factors that are not of primary importance, as demonstrated by comparison with more sophisticated models. By its emphasis on the relevant factors the model is informative and useful for extensions to more complex cases.

ACKNOWLEDGMENTS

The author is grateful to Dr. D. Baeriswyl for many valuable conversations which helped him to understand the theoretical aspects of soliton excitations. He is particularly in debt to Professor J.-M. André, Professor W. Baltensperger, Dr. J. Broz, and Professor H.-D. Försterling for stimulating discussions.

APPENDIX: NUMERICAL PROCEDURE

The potential consists of N piecewise constant steps. The wave amplitude and the corresponding derivative for the wave function within step i between the discontinuities x_i and x_{i+1} are given by[40] (a) for $\epsilon > \delta_i$,

$$\Psi_i = A_i \sin k_i(x-\bar{x}_i) + B_i \cos k_i(x-\bar{x}_i) ,$$

$$\frac{\partial}{\partial x}\Psi_i = A_i k_i \cos k_i(x-\bar{x}_i) - B_i k_i \sin k_i(x-\bar{x}_i) ;$$

(b) for $\epsilon < \delta_i$,

$$\Psi_i = A_i \sinh \kappa_i(x-\bar{x}_i) + B_i \cosh \kappa_i(x-\bar{x}_i) ,$$

$$\frac{\partial}{\partial x}\Psi_i = A_i \kappa_i \cosh \kappa_i(x-\bar{x}_i) + B_i \kappa_i \sinh \kappa_i(x-\bar{x}_i) ;$$

(c) for $\epsilon = \delta_i$,

$$\Psi_i = B_i ,$$

$$\frac{\partial}{\partial x}\Psi_i = 0 ,$$

where $k_i = \sqrt{\epsilon - \delta_i}$ and $\kappa_i = \sqrt{\delta_i - \epsilon}$ are the dimensionless wave vectors with energy $\epsilon = E/\hbar^2/2ma^2$ above and below the potential $\delta_i = V_i/\hbar^2/2ma^2$, respectively. The coefficients A_i, B_i have to be determined solving an eigenvalue problem.[41] [$a = 1.40$ Å, $l_i = x_{i+1} - x_i$, and $\bar{x}_i = \frac{1}{2}(x_i + x_{i+1})$.] The equation

$$\begin{bmatrix} R_{i+1} \\ Q_{i+1} \end{bmatrix} = \underline{\tau}_i \begin{bmatrix} R_i \\ Q_i \end{bmatrix}$$

with the following matrices, (a) for $\epsilon > \delta_i$,

$$\underline{\tau}_i = \begin{bmatrix} \cos(k_i l_i) & (1/k_i)\sin(k_i l_i) \\ -k_i \sin(k_i l_i) & \cos(k_i l_i) \end{bmatrix} ,$$

(b) for $\epsilon < \delta_i$,

$$\underline{\tau}_i = \begin{bmatrix} \cosh(\kappa_i l_i) & (1/\kappa_i)\sinh(\kappa_i l_i) \\ \kappa_i \sinh(\kappa_i l_i) & \cosh(\kappa_i l_i) \end{bmatrix} ,$$

(c) for $\epsilon = \delta_i$,

$$\underline{\tau}_i = \begin{bmatrix} 1 & l_i \\ 0 & 1 \end{bmatrix} ,$$

transfers the wave amplitude at the discontinuity x_i,

$$R_i \equiv \Psi_{i-1}(x_i) = \Psi_i(x_i) ,$$

$$Q_i \equiv \frac{\partial}{\partial x}\Psi_{i-1}(x_i) = \frac{\partial}{\partial x}\Psi_i(x_i) ,$$

over the step i.[42]

The equation

$$\begin{bmatrix} R_{N+1} \\ Q_{N+1} \end{bmatrix} = \underline{T}(\epsilon) \begin{bmatrix} R_1 \\ Q_1 \end{bmatrix}$$

with

$$\underline{T}(\epsilon) = \prod_{i=1}^{N} \underline{\tau}_i \equiv \begin{bmatrix} a & b \\ c & d \end{bmatrix}$$

relates the wave amplitude at the left end of the first step x_1 with the wave amplitude at the right end of the last step x_{N+1}.

The eigenvalue problem

$$\underline{T}(\epsilon) \begin{bmatrix} R_1 \\ Q_1 \end{bmatrix} = \lambda(\epsilon) \begin{bmatrix} R_1 \\ Q_1 \end{bmatrix}$$

with the cyclic boundary condition of the ring

$$\begin{bmatrix} R_{N+1} \\ Q_{N+1} \end{bmatrix} = \begin{bmatrix} R_1 \\ Q_1 \end{bmatrix}$$

is solved with the eigenvalue $\lambda(\epsilon^m) = 1 = \frac{1}{2}(a+d)$.

The eigenvalue problem

$$\underline{T}(\epsilon) \begin{bmatrix} R_1 \\ Q_1 \end{bmatrix} = \lambda(\epsilon) \begin{bmatrix} R_1 \\ Q_1 \end{bmatrix}$$

with the "end-to-end" boundary condition of the chain $R_{N+1}=R_1=0$ is solved with the condition $b(\epsilon^m)=0$ and the eigenvalue $\lambda(\epsilon^m)=d$.

The coefficients A_i^m, B_i^m for the mth wave function with the energy ϵ^m and valid within step i are given by (a) for $\epsilon^m > \delta_i$,

$$\begin{bmatrix} A_i^m \\ B_i^m \end{bmatrix} = \begin{bmatrix} -\sin(\frac{1}{2}k_i^m l_i) & (1/k_i^m)\cos(\frac{1}{2}k_i^m l_i) \\ \cos(\frac{1}{2}k_i^m l_i) & (1/k_i^m)\sin(\frac{1}{2}k_i^m l_i) \end{bmatrix} \begin{bmatrix} R_i^m \\ Q_i^m \end{bmatrix};$$

(b) for $\epsilon^m < \delta_i$,

$$\begin{bmatrix} A_i^m \\ B_i^m \end{bmatrix} = \begin{bmatrix} \sinh(\frac{1}{2}\kappa_i^m l_i) & (1/\kappa_i^m)\cosh\frac{1}{2}\kappa_i^m l_i) \\ \cosh(\frac{1}{2}\kappa_i^m l_i) & (1/\kappa_i^m)\sinh(\frac{1}{2}\kappa_i^m l_i) \end{bmatrix} \begin{bmatrix} R_i^m \\ Q_i^m \end{bmatrix};$$

(c) for $\epsilon^m=\delta_i$,

$$\begin{bmatrix} A_i^m \\ B_i^m \end{bmatrix} = \begin{bmatrix} 0 \\ R_i^m \end{bmatrix}.$$

This wave function is normalized and orthogonalized,

$$\sum_{i=1}^{N} \int_{x_i}^{x_{i+1}} \Psi_i^m(x)\Psi_i^{m'}(x)dx = \delta_{mm'}.$$

[1]W.-P. Su, J. R. Schrieffer, and A. J. Heeger, Phys. Rev. B **22**, 2099 (1980); B **28**, 1138(E) (1983).

[2]H. Takayama, Y. R. Lin-Liu, and K. Maki, Phys. Rev. B **21**, 2388 (1980).

[3]D. K. Campbell and A. R. Bishop, Nucl. Phys. B **200**, 297 (1982).

[4]S. R. Phillpot, D. Baeriswyl, A. R. Bishop, and P. S. Lomdahl, Phys. Rev. B **35**, 7533 (1987).

[5]D. Baeriswyl, in Theoretical Aspects of Band Structures and Electronic Properties of Pseudo-One-Dimensional Solids, edited by H. Kamimura (Reidel, Dordrecht, 1985), p. 1.

[6]D. Baeriswyl, G. Harbeke, H. Kiess, and W. Meyer, in *Electronic Properties of Polymers,* edited J. Mort and G. Pfister (Wiley, New York, 1982), Chap. 7.

[7]G. W. Bryant and A. J. Glick, Phys. Rev. B **26**, 5855 (1982).

[8]S. Roth and H. Bleier, Adv. Phys. **36**, 385 (1987).

[9]A. J. Heeger, S. Kivelson, J. R. Schrieffer, and W. -P. Su, Rev. Mod. Phys. **60**, 781 (1988).

[10]D. Baeriswyl and K. Maki, Phys. Rev. B **31**, 6633 (1985).

[11]P. Horsch, Phys. Rev. B **24**, 7351 (1981).

[12]S. Kivelson, W.-P. Su, J. R. Schrieffer, and A. J. Heeger, Phys. Rev. Lett. **58**, 1899 (1987).

[13]S. N. Dixit and S. Mazumdar, Phys. Rev. B **29**, 1824 (1984).

[14]V. Heine, in *Solid State Physics,* edited by H. Ehrenreich, F. Seitz, and D. Turnbull (Academic, New York, 1980), Vol. 35, p. 1.

[15]F. Bär, W. Huber, G. Handschig, H. Martin, F. Schäfer, and H. Kuhn, J. Chem. Phys. **32**, 467 (1960).

[16]F. F. Seelig and H. Kuhn, Z. Naturforsch. **18a**, 1191 (1963).

[17]H.-D. Försterling, W. Huber, and H. Kuhn, Int. J. Quantum Chem. **1**, 225 (1967).

[18]H. Kuhn, Angew. Chem. **69**, 239 (1957).

[19]H. Kuhn, W. Huber, and F. Bär, in *Calcul des Fonctions d'Onde Moléculaire* (Edition du Centre National de la Recherche Scientifique, Paris, 1958), p. 179.

[20]H.-D. Försteling, W. Huber, H. Kuhn, H. H. Martin, A. Schweig, F. F. Seelig, and W. Stratmann, in *Optische Anregung Organischer Systeme,* edited by W. Foerst (Verlag Chemie, Weinheim, 1966), p. 55.

[21]H. Kuhn, Chimia. **4**, 203 (1950).

[22]R. E. Peierls, *Quantum Theory of Solids* (Clarendon, Oxford, 1955), p. 108.

[23]H.-D. Försterling and H. Kuhn, *Moleküle und Molekülanhäufungen Einführung in die Physikalische Chemie* (Springer, Berlin, 1981), p. 90.

[24]J. M. Ziman, *Solid State Physics,* edited by H. Ehrenreich, F. Seitz, and D. Turnbull (Academic, New York, 1971), Vol. 24, p. 1.

[25]N. W. Ashcroft, J. Phys. C **1**, 232 (1968).

[26]I. Abarenkov and V. Heine, Philos. Mag. **12**, 529 (1965).

[27]D. S. Boudreaux, R. R. Chance, J. L. Brédas, and R. Silbey, Phys. Rev. B **28**, 6927 (1983).

[28]H. Martin, H.-D. Försterling, and H. Kuhn, Tetrahedron Suppl. 2 **19**, 243 (1963).

[29]A. Almenningen, C. Bastiansen, and M. Traetteberg, Acta Chem. Scand. **12**, 1221 (1958).

[30]B. P. Stoicheff, Can. J. Phys. **32**, 339 (1954).

[31]Equation (2), $\rho a = 1.00 - 10.2(d/a-1) + 35.0(d/a-1)^2$, may be compared with the self-consistency relation obtained from the two-dimensional pseudopotential model (Ref. 17): $\rho a^2 = 1.00 - 12.86(d/a-1) + 102.02(d/a-1)^2$, and with the correlation bond order p vs bond length within the Hückel model (Ref. 39): $p\pi/2 = 0.96 - 10.35(d/a-1) + 41.04(d/a-1)^2$. The agreement between calculated and measured bond lengths of π-electron systems is a good measure of the quality of the model used. It has been shown that the quality of the two-dimensional pseudopotential model has to be valued higher than the LCAO method in that respect (Ref. 39).

[32]As shown in Secs. III C and III D, the value $\alpha=1.95$ [Eq. (3)] extracted from the model of Ref. 28 leads to the result, in agreement with experiment, that the 18-annulene is the first to show beginning bond-length alternation and that polyacetylene has bond-length alternation of 0.08 Å with a bond gap of 1.34 eV. However, the absorption limit of polyenes is at longer wavelengths than observed [polyene $n=15$: $\lambda=504$ nm (experimental), $\lambda=676$ nm (theoretical) with electron correlation (Ref. 20) taken into account]. Agreement between the theoretical and experimental λ values of polyenes is obtained with $\alpha=2.15$. With this value the 14-annulene is the first to show beginning bond-length alternation and the band gap of polyacetylene is 2.2 eV.

[33]J. Delhalle, J. L. Brédas, and J.-M. André, Chem. Phys. Lett. **78**, 93 (1981).

[34]C. A. Coulson and W. T. Dixon, Tetrahedron **17**, 215 (1962).

[35]H. C. Longuet-Higgins and L. Salem, Proc. R. Soc. London, Ser. A **251**, 172 (1959).

[36]L. M. Jackson, F. Sondheimer, Y. Amiel, D. A. Ben-Efraim, J. Gaoni, R. Wolovski, and A. Bothner-By, J. Am. Chem. Soc. **84**, 4307 (1962).

[37]J. B. Lando and M. K. Thakur, *Molecular Electronic Devices II,* edited by F. L. Carter (Dekker, New York, 1987), p. 237.
[38]S. Kivelson and W.-K. Wu, Phys. Rev. B **34**, 5423 (1986).
[39]H. D. Försterling and H. Kuhn, Z. Naturforsch, **22a**, 1204 (1967).
[40]E. O. Kane, in *Tunneling Phenomena in Solids,* edited by E. Burstein and S. Lundqvist (Plenum, New York, 1969), p. 1.
[41]W. L. McCubbin and F. A. Teemull, Phys. Rev. A **6**, 2478 (1972).
[42]R. Tsu and L. Esaki, Appl. Phys. Lett. **22**, 562 (1973).
[43]Interestingly, while kinks may be trapped by the site defects, polarons may be trapped by bond defects (Ref. 4). This can be explained by considering the squares of the wave functions of the intergap states [Fig. 7(a)] showing the maxima and zeros at sites in case of the kink and at bonds in case of the polaron.
[44]The curves connecting the density values at the middle of bonds of the intergap states of the polaron [circles in Fig. 7(a), negative-polaron case] agree with the envelopes calculated within the continuum limit of the SSH model (Ref. 3, Eqs. 3.8b and 3.8c), but are obviously not envelopes in the present model.